Lauric Acid-Induced Formation of a Lyotropic Nematic Phase of Disk-Shaped Micelles

Giuseppe Colafemmina,[†] Raffaella Recchia,[†] Andrea S. Ferrante,[‡] Samiul Amin,[§] and Gerardo Palazzo*,[†]

Dipartimento di Chimica, Università di Bari, and CSGI, via Orabona 4, 70126-bari, Italy, Unilever R&D, Port Sunlight Laboratories, Quarry Road East, Bebington Wirral CH63 3JW, United Kingdom, and Malvern Instruments Limited, Grovewood Road, Malvern WR14 1XZ, United Kingdom

Received: March 8, 2010; Revised Manuscript Received: April 23, 2010

Addition of small amounts of lauric acid (LA) to a micellar solution of sodium dodecyl sulfate (SDS, 11.5 wt %) and cocamidopropyl betaine (CAPB, 3 wt %) has a dramatic effect on the rheological properties and phase behavior of the system. The viscosity increases by more than 1 order of magnitude up to a weight ratio LA/SDS = 0.17 and decreases for further LA loading. The decrease in viscosity is associated with the formation of a birefringent liquid crystalline phase. The evolution of the system from isotropic micelles in the absence of LA to lyotropic liquid crystals up to a weight ratio LA/SDS = 0.30 was probed by a combination of ^{23}Na NMR quadrupolar splitting, measurements of water and surfactant self-diffusion coefficients via ^{1}H-PGSE-NMR, and rheology. The evolution of the water self-diffusion coefficients indicates that LA induced a dramatic increase in the anisotropy of disk-shaped micelles. Birefringent samples always showed a well developed ^{23}Na quadrupolar splitting with a line shape typical of monodomain samples. This suggests that the whole sample is easily oriented within the spectrometer electromagnet, as usually observed for nematic liquid crystals. Sample spinning first destroys the alignment (only a single peak is discernible in the ^{23}Na NMR spectrum). Then, upon prolonged spinning, the alignment develops again. This indicates that the system is composed by disklike micelles aligning themselves with their normal perpendicular to the magnetic field. On the other hand, the linear viscoelastic response close to the nematic transition shows features usually observed in wormlike micellar systems (e.g., nearly Maxwellian behavior). To reconciliate the rheological data and the NMR evidence of disklike micelles, the formation of columnar stacks of disklike micelles is proposed. The rheology of the isotropic phase can therefore be interpreted in terms of entanglements of "living columnar stacks" of disklike micelles, and the nematic phase observed at high LA content could be attributed to a nematic columnar phase N_{Col} formed by the alignment of such stacks.

1. Introduction

Surfactants in water self-assemble forming micelles and other aggregates. The equilibrium shape and size of these aggregates can be rationalized in terms of the free energy cost to be paid to bend the surfactant film away from its optimal curvature H_0. In the most common case of uniform composition of the surfactant film (H_0 constant over the aggregate surface), geometrical arguments are sufficient to predict the size distribution of the self-assembled aggregates.[1] Spherical micelles are expected to be relatively monodisperse while, when H_0 favors cylindrical shape, the requirement of minimizing the unfavorable hemispherical end-caps leads to the formation of highly polydisperse giant wormlike micelles. On the other hand, if $H_0 = 0$ (as in disklike aggregates) the number of molecules residing on the unfavorable rims grows with aggregate size and this leads to the formation of infinite aggregates, i.e., to phase separation of a true lamellar phase.[1] Accordingly, for a large number of surfactant systems the tuning of intensive variables such as T or composition results in a transition among isotropic solutions of spherical and wormlike micelles and lamellar mesophases. For concentrated systems, excluded volume interactions start to play a main role and lyotropic mesophases based on long-range ordered spherical and cylindrical objects naturally appears (viz. disconnected cubic phases, calamitic nematic and hexagonal phases). In view of that, the realm of the *isotropic* micellar system is dominated by spherical and wormlike aggregates, the latter being characterized by very interesting viscoelastic properties (reminiscent of their polymer-like structure) and by an isotropic-to-nematic transition that often takes place at very low volume fraction (depending on the micelles' aspect ratio). However, in addition to the two common cases mentioned above, thermodynamic stable solutions of discrete disklike aggregates (disklike micelles) also exist.[2] This requires that the spontaneous curvatures in the middle and in the edges of the aggregates are different, suggesting a different chemical composition of the surfactant film. Accordingly, most of the recipes to form disklike micelles involve two or more amphiphiles. Also the behavior of a nominally two components system, such as cesium pentadecafluorooctanoate and water can be traced out to heterogeneities in the local chemical composition because the Cs^{2+} ion is preferentially adsorbed on the "planar" caps rather than the "curved" rims of the micelles.[3] The stringent requirement of suitable different spontaneous curvatures in different regions of the aggregates implies that, in surfactant systems, disklike micelles are relatively uncommon compared to spherical and wormlike micelles.

For volume fractions high enough, the competition between packing and orientational entropy brings to the spontaneous

* Corresponding author. Fax: 39 0805442129. Tel: 39 0805442028. E-mail: palazzo@chimica.uniba.it.
[†] Università di Bari and CSGI.
[‡] Unilever R&D. E-mail: Andrea.Ferrante@Unilever.com.
[§] Malvern Instruments Limited. E-mail: Samiul.Amin@malvern.com.

10.1021/jp1020774
Published on Web 05/12/2010

orientation of the discs and to the formation of a discotic nematic phase N_D according to a mechanism analogous to that taking place in the case of rods. Other liquid crystalline mesophases based on disks are also possible, in analogy to the thermotropic liquid crystals formed by disklike molecules.[4,5] We will return to this issue in the discussion section.

Classical formulations giving rise to discotic nematics (beside the aforementioned cesium pentadecafluorooctanoate−water) involve the mixture of a long chain alcohol with a surfactant in water or brine (see the review by Forrest and Reeves[2] for a list of the formulations). The two cases most studied in the literature are the sodium dodecyl (or decyl) sulfate with decanol in water or D_2O,[6,7] or potassium laurate with decanol in water.[8,9] In both cases a variety of phases have been observed, including a discotic nematic phase N_D. Another case of disklike micelle formation involves sodium dodecyl sulfate (SDS) with a strongly binding organic counterion.[10] Lately, the use of disklike micelles made by mixtures of phospholipids with different packing properties has become popular in the field of structural biology where they are known as "bicelles" (bilayer-based micelles).[11,12] While the structure of many isotropic and nematic systems based on disk-shaped micelles has been investigated in detail by means of NMR techniques,[13–18] detailed studies on the rheology of these systems are lacking, since rheological measurements are usually not reported (with one notable exception[10]). In this contribution, we examine the effect of small quantities of lauric acid (LA) on the self-assembling of mixed micelles formed by SDS and cocamide propyl betaine (CAPB). As will be detailed in the Results, doping the SDS/CAPB with lauric acid confers the characteristic viscoelastic behavior of a nearly Maxwellian liquid (e.g., presenting a single relaxation time), which usually is associated with the presence of wormlike micelles but the detailed analysis of the water and surfactant self-diffusion coefficients indicate that the micelles can only be described properly as oblate micelle (disks). For LA content high enough the system becomes a birefringent nematic phase that can be easily oriented in a magnetic field. Again thse are features common to calamitic nematics based on wormlike micelles but the response of the ^{23}Na NMR spectrum to sample spinning clearly indicates the disklike nature of the micelles in this phase. The Discussion is focused on how to resolve the apparent contradiction between the evidence fron NMR and rheological measurements.

2. Materials and Methods

Sodium dodecyl sulfate (SDS) was purchased from SIGMA Chemical Co.; lauric acid (Prifac 2922) was purchased from Uniqema, and cocamidopropyl betaine (Tegobetain ck) was purchased from Evonik Goldschmidt GmbH as a 30% aqueous solution (the Tegobetain solution contains about 7% wt of NaCl, as indicated by conductivity measurements).[19] All these chemicals have been used as received; the water was twice distilled.

The composition range explored in the present work corresponds to the loading of lauric acid (LA) to SDS (11.5 wt %) and cocamidopropyl betaine (CAPB, 3.0 wt %) aqueous solutions. This was accomplished by mixing in suitable ratios two stock solutions at pH = 6.0: one without LA and the other with the highest LA content. The latter solution was prepared by adding molten lauric acid to a warm (60 °C) solution of SDS and CAPB. The resulting solution was then stirred for several hours at 60 °C and then allowed to reach room temperature. It should be noticed that SDS alone (i.e., without CAPB) does not form a single phase mixture with LA (LA precipitates). The mixture was then titrated to pH = 6.0 with NaOH and finally water was added to reach the following composition: LA = 3.5 wt %, SDS = 11.5 wt %, CAPB = 3.0 wt %.

Routine viscosity measurements have been carried out using a vibrational viscometer SV-10 (A&D) at room temperature (23 ± 1 °C). The natural frequency of the vibrating elements is 30 s^{-1}, and the response of this sort of instrument furnishes the true (zero shear) viscosity only for a Newtonian fluid. For a non-Newtonian fluid, the instrument measures the value of the complex viscosity at the frequency of operation. Only for extremely low frequencies does this value correspond to the zero shear viscosity. In case the fluid obeys a Cox−Merz relation, the value obtained gives the viscosity at a finite shear rate, given by the frequency. However, the technique used in this study has allowed us to qualitatively follow trends in the viscosity. To carry out detailed rheological characterizations, samples at selected compositions have been investigated through a controlled stress rheometer (Bohlin Gemini HR Nano-Malvern Instruments). All measurements were carried out using a cone and plate geometry, and the temperature was kept constant at 25 °C.

Self-diffusion coefficient measurements have been carried out by the Fourier transform NMR pulsed field gradient spin−echo (PGSE-NMR) method.[20] Experiments were performed on a BS-587A NMR spectrometer based on an electromagnet (Tesla), operating at 80 MHz for the proton. The spectrometer was equipped with a pulsed field gradient unit (Autodif 504, STELAR s.n.c.). The pulse sequence employed was the Stejskal−Tanner sequence,[21] 90°−τ−180°−τ−echo, with two rectangular field gradient pulses 0.04 T m^{-1} and variable duration, separated by a constant interval Δ = 140 ms. The magnetic field was locked by an external D_2O lock signal for all the samples. The temperature of the samples was maintained at 298.0 ± 0.2 K by means of a built-in variable temperature control unit.

The sodium-23 NMR spectra have been collected using the same spectrometer using 20 kHz as spectral width and a 10 μs pulse. The ^{23}Na spectra were acquired with 32−64 scans and subsequently Fourier Transformed with a line broadening of 10 Hz.

For the calculation of the micellar volume fraction a density of 1 mg cm^{-3} was assumed for all the components.

3. Results

3.1. General Features of the System. The solution formed by SDS 11.5 wt % and CAPB 3.0 wt % in water is a slightly viscous isotropic liquid.

Addition of small amounts of lauric acid (LA) to a solution of SDS 11.5 wt % and CAPB 3.0 wt % in water induces dramatic changes in the rheological properties of the system. The apparent viscosity (measured by means of the vibro-viscometer) increases until the lauric acid concentration reaches 2 wt % (Figure 1).[22] At higher LA content the apparent viscosity decreases notably but it never reaches the values of the samples without LA. These trends in viscosity have been confirmed by more accurate measurements of flow curves by means of a conventional rheometer (the trend can be observed by accurate examination of the flow curves presented in Figure 2). Observation through crossed polarizers reveals that the samples with LA content higher than 2.7% are birefringent, and this suggests that the decrease of the viscosity can be due to a phase transition from a highly viscous but still isotropic micelle solution to a lyotropic liquid crystalline mesophase.

3.2. Rheological Properties. The dramatic change in the apparent viscosity observed upon very small addition of LA

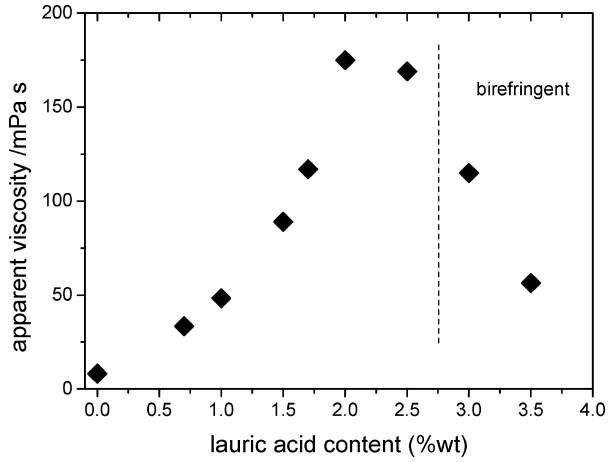

Figure 1. Apparent viscosity at $T = 23$ °C measured by means of the vibroviscosimeter for samples at fixed SDS (11.5 wt %) and CAPB (3.0 wt %) content and variable LA loading (pH = 6.0). The dashed line denotes the boundary between isotropic and birefringent regions.

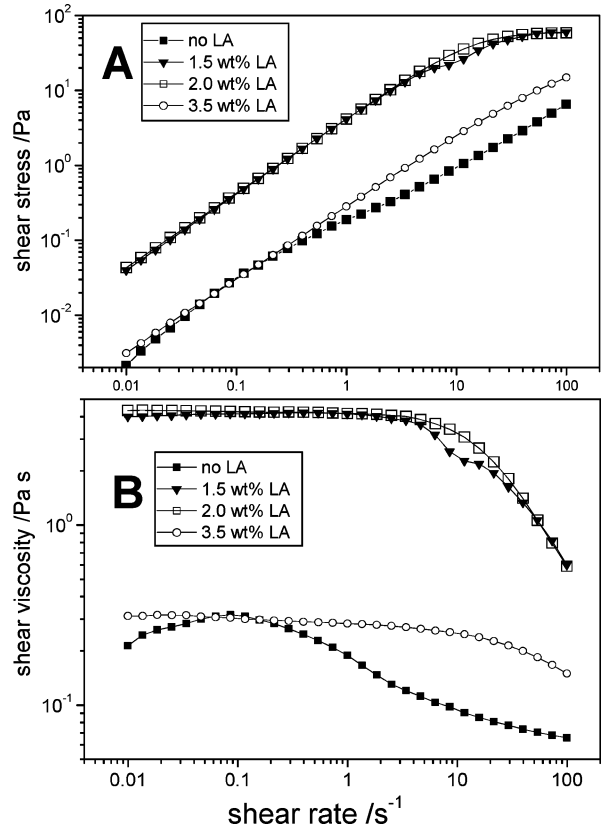

Figure 2. Nonlinear rheology experiments for samples at fixed SDS (11.5 wt %) and CAPB (3.0 wt %) content and four different LA loadings (pH = 6.0). (A) Flow curves (shear stress vs shear rate). (B) Shear viscosity as a function of the shear rate.

deserves a more detailed rheological investigation. Figure 2 shows the results for the flow curves obtained on four samples at different LA content: 0 wt % (i.e., micelles formed only by SDS and CAPB), 1.5 wt %, 2.0 wt % (i.e., close to the maximum in apparent viscosity), and 3.5 wt % (this last sample is birefringent). In the absence of LA, the system behaves as expected for a solution of small micelles; e.g., it shows low viscosity (Figure 2B) and the flow curve does not present any indication of a shear banding plateau (Figure 2A). The system, however, is slightly shear thickening at low shear rates and

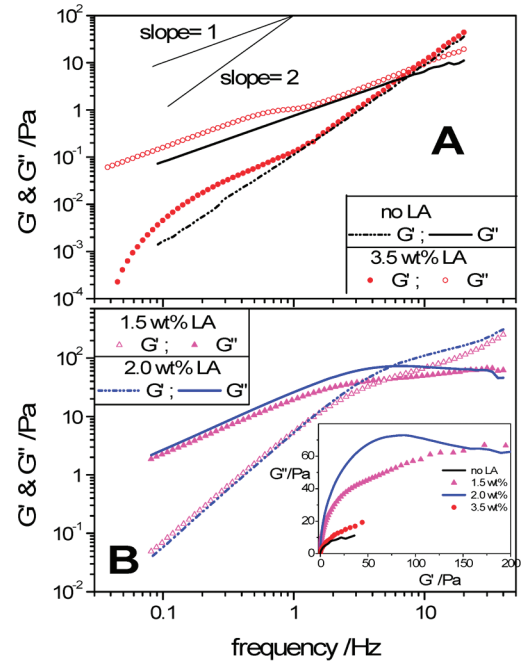

Figure 3. Elastic (G') and loss (G'') modulii from oscillatory measurements. In all the cases the SDS and CAPB contents were 11.5 and 3.0 wt %, respectively. (A) Samples without LA (black lines) and with 3.5 wt % LA (red dots). The latter sample is birefringent. (B) Solutions with 2.0 wt % LA (blue lines) and with 1.5 wt % LA (pink triangles). Inset: Cole−Cole plots for all the formulations.

becomes shear thinning for $\dot{\gamma} > 0.1$ s^{-1}. Small addition of LA (viz. 1.5 and 2.0 wt %) drastically changes the rheological features of the system. The LA loading induces a more than 1 order of magnitude rise in the viscosity (Figure 2B) and the flow curves show shear banding plateaus at high shear rates (Figure 2A).

On further addition of LA (3.5 wt % the birefringent sample) the viscosity drops and the shear banding plateau disappears so that the response to the flow is almost Newtonian, with shear thinning starting only at high shear rates. The lower viscosity observed at higher LA content is an indication of the transition to a nematic phase.

Figure 3 shows the results of oscillatory measurements on the very same samples. Addition of LA to the SDS/CAPB system also has a pronounced effect on the viscoelastic response of the fluid. In the absence of LA, the response is essentially dominated by the viscous modulus G'' with a crossover with the elastic modulus G' occurring at high frequencies. The frequency dependence of the G' and G'' also follows the typical ω and ω^2 scaling expected of a simple viscoelastic fluid composed of spherical micelles.

The G', G'' response drastically changes on addition of 1.5% LA. The viscous modulus G'' shows a clear maximum and the elastic modulus G' starts dominating at much lower frequencies than observed for the sample without LA. The absolute magnitudes of both G' and G'' are both considerably higher than for the sample without LA. At 2.0 wt % LA, the response is also very similar to that observed for the 1.5 wt % sample, except that G' seems to exhibit a more well-defined decrease after the crossover with G''. This behavior of G', G'' is reminiscent of the single element Maxwell fluid response typically exhibited by wormlike micelles.[23,24] The Maxwell type response can be more clearly seen by plotting a Cole−Cole plot, i.e., a plot of G'' vs G'. This has been carried out for the four samples and is plotted in the inset of Figure 3B. A pure single

element Maxwell model fluid exhibits a semicircular Cole−Cole plot. As seen in the inset of Figure 3B, only the sample with 2.0 wt % LA tends to exhibit this semicircular shape to a certain extent, while the other samples do not. This behavior again is reminiscent of the rheological behavior of wormlike micelles as evolution of a semicircular Cole−Cole signature through tuning of a compositional parameter and later deviations from a pure semicircular shape especially at high frequencies, as has been observed in numerous wormlike micelle systems.[25] It has been attributed to a different degree of entanglement of the wormlike micelles (incipient vs well developed) or to the presence of other relaxation mechanisms occurring at higher frequencies (short times), such as Rouse modes or the onset of branching.[25] On addition of even higher amounts of LA, the response of G' and G'' becomes again indicative of a fluidlike behavior of $G' < G''$ in a wide range of frequencies and is overall pretty similar to the viscoelastic response of the suspension without LA (apart from the strong deviation observed at lower frequencies). A relaxation time τ can be inferred from the crossover of G' and G''. The longest relaxation times τ (evaluated from the frequency at which $G' = G''$) also exhibit a maximum as a function of the LA loading. It is around 21 ms in the absence of LA and then increases to 29 ms at 1.5 wt % LA and remains at about 29 ms at 2.0 wt % LA. Further addition of LA (3.5 wt %) causes the drop of τ to the value (19 ms) similar to that observed in absence of LA.

The rheological phenomenology shown in Figures 1−3 is often observed in solutions of wormlike micelles.[26] In this case, phenomena such as shear banding, the presence of a sizable viscosity maximum and the evolution of a single element Maxwell fluid type viscoelastic response upon tuning composition are often considered evidence for the presence of wormlike micelles. At first glance, one would be also tempted to attribute the rheological behavior here observed to the formation of wormlike micelles, since a previous study of mixed micelles of SDS with CAPB in different proportions has shown evidence of the growth of elongated, rodlike micelles.[19] However, the spectroscopic investigations described in the following sections clearly demonstrate the absence of rod- or wormlike micelles, indicating that the situation is much more delicate.

3.3. ^{23}Na NMR: Structure of the Lyotropic Liquid Crystals. It has been mentioned previously that for LA content larger than 2.7 wt % the system shows birefringence, implying the existence of liquid crystalline mesophases. However, the presence of birefringence alone does not exclude the possible coexistence of isotropic and liquid crystalline phases (or of two mesophases); therefore, the nature of the birefringent samples was investigated through ^{23}Na NMR. In the case of quadrupolar nuclei in the presence of an electric field gradient, the degeneracy of the Zeeman transitions is lifted to give $2I$ transitions ($I > {}^1/_2$ is the spin quantum number). In the case of sodium-23 ($I = {}^3/_2$) this means three equidistant NMR transitions. In the isotropic case, all three transitions are degenerate in energy and thus overlap in the NMR spectrum, reflecting a null average electric field gradient. In anisotropic liquid crystals the quadrupolar interaction tensor is incompletely averaged. The separation of the outer components (satellites) of the triplet depends on the electric quadrupolar moment (eQ) and on the electric field gradient (eq) as[27]

$$2\Delta\nu = \frac{e^2qQ}{h}\frac{(3\cos^2\vartheta - 1)}{2} \qquad (1)$$

where ϑ is the angle between the magnetic field $\mathbf{B_0}$ and the direction of the electric field gradient q. For a *perfect* fully oriented charged phase (ϑ = constant over the sample), the ^{23}Na NMR spectrum of sodium ions has three lines separated by $\Delta\nu$ and in a 3:4:3 intensity ratio. For liquid crystalline phases, eq 1 is usually rewritten in terms of the angle Ω between the director and the magnetic field direction as

$$2\Delta\nu = \frac{e^2qQ}{h}S_{ZZ}\frac{(3\cos^2\Omega - 1)}{2} \qquad (2)$$

where S_{zz} is the degree of order of the electric field gradient with respect to the director. Note that the separation of peaks decreases by a factor 2 in going from parallel $\Omega = 0$ to perpendicular $\Omega = \pi/2$ orientation of the director with respect to $\mathbf{B_0}$. For a polycrystalline or powder sample, the random three-dimensional distribution of Ω angles within the sample leads to a powder type spectrum characterized by a narrow high central peak (all orientations contribute to this transition) and two broad tails each characterized by a small peak (due to the $\Omega = 90°$ orientations) and a very weak shoulder (due to the unique Ω=0° orientations).[28]

All the samples that are optically isotropic reveal a single ^{23}Na NMR peak, thus confirming the isotropic nature of the micellar solution. For all the birefringent samples (i.e., LA content >2.7 wt %) the ^{23}Na NMR spectrum reveals the three sharp peaks with integral ratio 3:4:3 diagnostic of a single crystal orientation (see the upper panel of Figure 4 for a representative spectrum). This means that the sample successfully and very rapidly oriented itself under the effect of the magnetic field. Furthermore, they are single phase systems because only *one* triplet is observed and the intensity ratio among peaks is the canonical 3:4:3; in the presence of additional isotropic phases, their sodium ions should contribute to the central peak, thus changing the ratio. Discrete nonspherical micelles at high enough concentration can orient themselves along a preferred orientation, giving raise to lyotropic liquid crystals. In most of the cases only orientational order is achieved and the liquid crystal is a nematic one. In analogy with thermotropic liquid crystals one distinguishes discotic (based on disklike micelles) and calamitic (based on rod-shaped micelles) nematics. In the former the nematic director is defined by the normal to the disk plane while in the latter it is defined by the long axis of the rod. Being formed by finite objects, these phases usually possess a low viscosity and, when exposed to a strong magnetic field, the magnetic torques can efficiently orient the whole sample to give a single crystal in a relatively short time (from a few seconds to 1 day depending on the system and on the magnetic field). Accordingly, the spectrum of Figure 4 indicates that the birefringent phase formed for LA loading larger than 2.7% phase is a nematic liquid crystalline phase. The final orientation depends on the magnetic properties of the surfactants and in particular on the anisotropy of diamagnetic susceptibility $\Delta\chi$.[29] Surfactants with aliphatic tails have usually negative $\Delta\chi$ while the presence of phenyl moieties confers a positive $\Delta\chi$.[30] One distinguishes between nematic of type I that orients with the director parallel to the applied magnetic field $\mathbf{B_0}$ and nematic of type II that orients with the director perpendicular to $\mathbf{B_0}$.[2] In the present case ($\Delta\chi < 0$; surfactants with aliphatic tails), the minimum energy orientation is where the magnetic field is perpendicular to the surfactant long axis; i.e., for rodlike micelles the micelle long axis is parallel to $\mathbf{B_0}$ while for disklike micelles the normal to the disk is perpendicular to $\mathbf{B_0}$.[2] Accordingly, a way to discriminate between calamitic and discotic nematics is

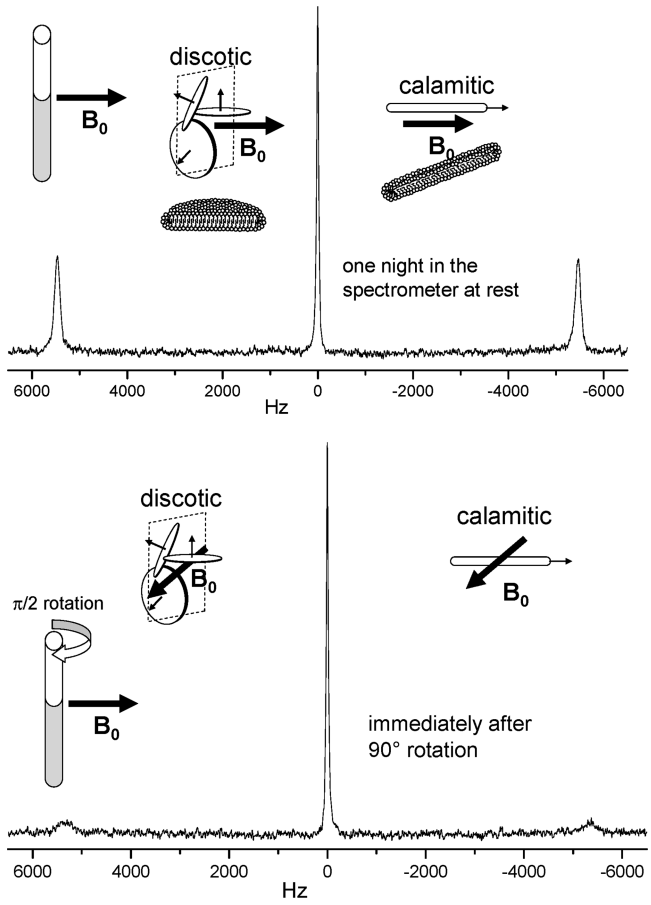

Figure 4. ^{23}Na NMR spectrum of a birefringent sample; conditions: $T = 25$ °C, the formulation is SDS 11.5 wt %, CAPB 3.0 wt %, and LA 3.0 wt % (pH = 6.0). The relative orientation of the magnetic field $\mathbf{B_0}$ with respect to the NMR tube is schematized in the far left of the panels. Upper panel: sample after one night at rest within the electromagnet. The quadrupolar splitting corresponding to a single crystal orientation is evident. Also shown, as cartoons, are the orientation expected for rodlike (right) and disklike (left) micelles forming calamitic and discotic nematics, respectively. Note that in the case of discotic nematic there are infinite directions perpendicular to $\mathbf{B_0}$. Lower panel: spectrum collected immediately after a 90° rotation of the NMR tube. The relative orientation of $\mathbf{B_0}$ and the liquid crystal directors are schematized in the case of calamitic (right) and discotic (left) nematics.

to probe the reorientation induced by changes in the $\mathbf{B_0}$ direction[31] exploiting the geometry of an NMR spectrometer based on electromagnet. With this setup the magnetic field $\mathbf{B_0}$ is normal to the spinning axis (long axis of the NMR tube). The sample was placed in the electromagnet overnight, permitting the nematic microdomains to align to the orientation that minimizes the energy of the system. As sketched in Figure 4, in the case of a calamitic nematic the cylindrical micelles will align along $\mathbf{B_0}$ while in the case of a discotic nematic the disklike micelles will align with their normal lying in the plane perpendicular to $\mathbf{B_0}$ (note that in this case there are infinite orientations lying on the plane perpendicular to $\mathbf{B_0}$). Then the tube was suddenly rotated by 90° and ^{23}Na NMR spectrum rapidly recorded. Just after the rotation the micelles preserve their orientation relative to the NMR tube, and this results in a net 90° rotation of $\mathbf{B_0}$. Therefore, after rotation, the directors will be all normal to $\mathbf{B_0}$ in the case of a calamitic nematic, while they will be spread out randomly in a plane containing $\mathbf{B_0}$ in the case of a discotic nematic (the so-called two-dimensional powder). According to eq 2, this means that for a calamitic

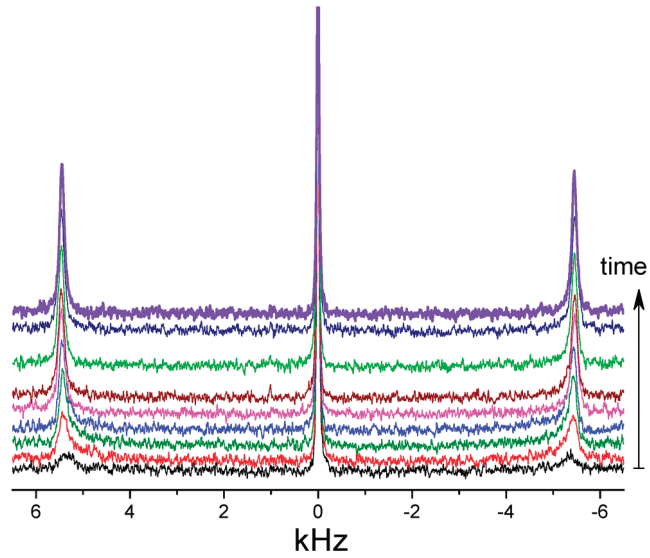

Figure 5. Reorientation kinetics of the nematic phase (same sample of Figure 4). ^{23}Na NMR spectra collected at different times after the start of the spinning. The spectra have been arbitrarily shifted along the vertical axis for the sake of readability. The spectrum recorded immediately after the rotation is at the bottom.

nematic the splitting measured immediately after rotation will be half that measured after a long time, while the intensities are unchanged.

On the other hand, for discotic nematic the random orientation of directors corresponds to a nonmonotonic NMR spectral density $\propto [\sin(2\Omega)]^{-1} = [\sin(2\cos^{-1}((2\nu/\Delta\nu + 1)/3)]^{-1}$. The corresponding broad spectrum (2D powder pattern) is dominated by the central peak and four satellites corresponding to the discontinuities at $\pm 2\Delta\nu$ and $\pm\Delta\nu$. Experimentally (Figure 4), the 90° rotation of the sample does not result in the splitting halving, and this excludes the presence of calamitic nematic. Instead, the spectrum is strongly broadened and shows two very small satellites of unchanged splitting. Such a line shape could be compatible with the discotic nematic if two further satellites with twice that splitting are present. Unfortunately, our setup has a maximum spectral width of 20 kHz and the presence of these hypothetical peaks cannot be confirmed. To obtain a definitive evidence of the disk-shaped nature of the micelles forming the liquid crystal phase, the evolution of ^{23}Na NMR spectrum was probed under continuous spinning. After equilibration overnight, the NMR tube was spun at constant rate (37 Hz) and spectra were recorded every 5 min. Spinning calamitic nematic about an axis perpendicular to the field, destroys permanently the unique orientation giving the 2D powder pattern discussed above (strictly this is true above a critical spinning frequency, below such a value the splitting should depend on the rotation rate).[32] On the contrary, the spinning discotic nematic usually results first in the vanishing (broadening) of the satellites (due to the random orientation of nematics) but with time the splitting is recovered because the directors take up the unique direction perpendicular to $\mathbf{B_0}$ (along the spinning axis).[32] As shown in Figure 5A, spinning immediately broadens the satellites which, however, become sharper upon increasing the spinning time until the line shape of a fully oriented sample is recovered. This behavior definitively proves the disklike shape of the micelles forming this nematic phase. The fact that the quadrupolar splitting does not change during the reorientation suggests that the process does not involve a continuous reorientation of the microdomains directors but instead a discontinuous growth of the domains properly oriented (i.e., with

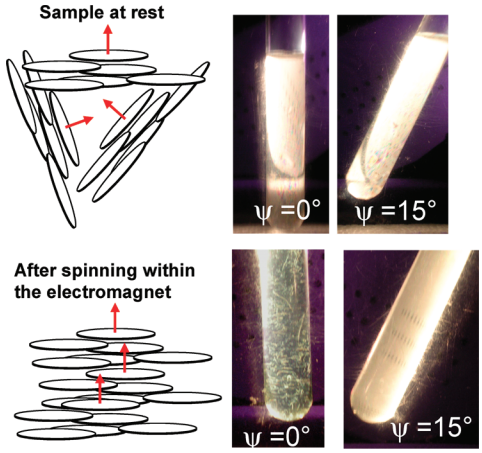

Figure 6. Appearance of the NMR tube between crossed polarizers (same sample of Figures 4 and 5). Upper panels: the freshly prepared sample shows birefringence independently from the orientation of the NMR tube. ψ denotes the angle between the long axis of the NMR tube and the polarizing plane (vertical). This reflects the microdomains structure schematized by the cartoon on the left. Lower panels: after extensive spinning in the electromagnet the sample appears isotropic when the tube is parallel to the polarizing plane but birefringent for other directions because it has the single crystal orientation schematized by the cartoon on the left.

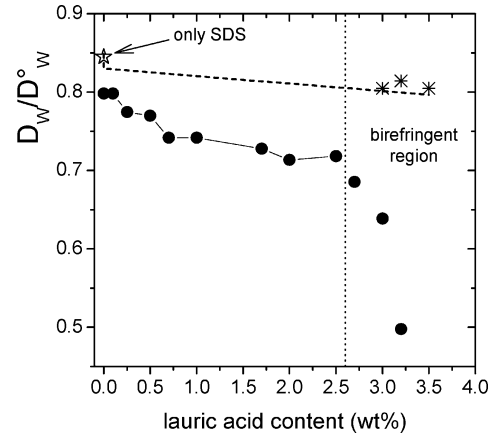

Figure 7. Reduced water self-diffusion coefficients at fixed SDS (11.5 wt %) and CAPB (3.0 wt %) content and variable LA loading (dots); also shown is the datum obtained for a water solution of only SDS 13 wt % (open star). The vertical dashed straight line is the boundary between isotropic and birefringent samples. For the birefringent samples the measured D_W depends on the time spent within the spectrometer (the long time values are denoted by asterisks). The dashed curve is the prediction according to the ECM for nonoblate micelles (eqs 4 and 5) assuming a constant hydration equal to that found for spherical SDS micelles (star). The solid curve represents the analysis according to the ECM for oblate micelles (see Appendix) with the same constant hydration but variable axial ratio of the micelles; the corresponding axial ratio values are shown in Figure 10. See text for details.

the director parallel to the spinning axis) at the expense of the other domains that, due to the rotation average, appear as randomly oriented. The time course of the reorientation as probed by the ratio between the intensities of the central and the satellites peaks is well described by a first-order kinetics and its characteristic time increases with the amount of lauric acid in the system passing from 3 min at 2.7 wt % LA to almost 1 h at 3.5 wt % LA (data not shown). Such a procedure strongly affects also the response of the sample to polarized light. Nonspun samples appear uniformly bright between crossed polarizers independently from the sample orientation (see Figure 6). On the contrary, after extensive spinning (i.e., after the single orientation pattern was recovered in the ^{23}Na NMR spectrum) the birefringence of the sample depends dramatically on the angle between the former spinning axis and the optical axis of the polarizer. Rotating the tube between the crossed-polarizers we pass from an almost isotropic sample (tube vertical or horizontal) to a strongly birefringent system (any other orientation), as shown in Figure 6, suggesting that the optical axis of the whole sample is now along the former spinning axis. As a whole, the results presented in this section indicate that the birefringent phase found at LA content larger than 2.7% is a nematic phase based on disklike micelles.

3.4. Water Diffusion. The microstructure of the isotropic solutions has been investigated by means of ^{1}H-PGSE NMR experiments and the subsequent analysis of the self-diffusion coefficients of water and surfactant. The diffusion of the surfactant will be discussed in the next section, here we anticipate that its self-diffusion coefficients are always very low (2 orders of magnitude below the corresponding diffusivities of water). The dependence of the water self-diffusion coefficients (D_W) on the lauric acid content is shown in Figure 7.

In Figure 7 the D_W values are normalized for the self-diffusion coefficient of pure water measured under the very same experimental condition; for comparison, the D_W measured in a solution 13 wt % of SDS in water (i.e., without CAPB) is also shown as an open star. In all the cases the measured D_W are systematically lower than the pure water diffusion. Basically, the observed decrease of the D_W/D^o_W ratio can be attributed to two mechanisms. The micelle excludes a fraction of the total volume for the diffusing molecule and this leads to a lengthening of the diffusion paths. This is often referred to as the "obstruction effect", and strongly affects also the diffusion of the micelles themselves. The second factor is related to specific interactions with the micellar wall. A fraction of the water is bound to the slow-diffusing micelles, and this leads to a further decrease in the measured self-diffusion coefficient.

These situations can be described through the so-called "effective cell model" (ECM).[33] The ECM gives a theoretical description of the molecular diffusion in a system of colloidal sized particles. The model is based upon the widely used concept of dividing a macroscopic system into small subsystems, or cells, in such a way that they together may represent the macroscopic properties. The reader is referred to ref 33 for a complete description of the model. The effective diffusion coefficient for a component i will, in this model, depend on both the diffusion of the cell and the diffusion within the cell. The equation for the total effective diffusion coefficient D_i of component i in a micellar system may be written as[34]

$$D_i = D_i^{\text{cell}}\left(1 - \frac{D_{\text{mic}}}{D_i^{\text{o}}}\right) + D_{\text{mic}} \qquad (3)$$

where D_i^{cell} is the effective self-diffusion coefficient in a cell centered on the micelle, D_i^{o} is the self-diffusion coefficient of component i in the bulk solution, and D_{mic} is the self-diffusion coefficient of the micelle. For water diffusion, D_i^{cell} is nearly the same as the measured total self-diffusion coefficient (D_W), because D_{mic} is very low. The key parameter of the model is the local variation of the product of the self-diffusion coefficient and the concentration of the component (C_iD_i). Simple cases are those where the cell is divided into two subvolumes. One subvolume is close to the micelle and is characterized by concentration C_1 and self-diffusion coefficient D_1, the rest of

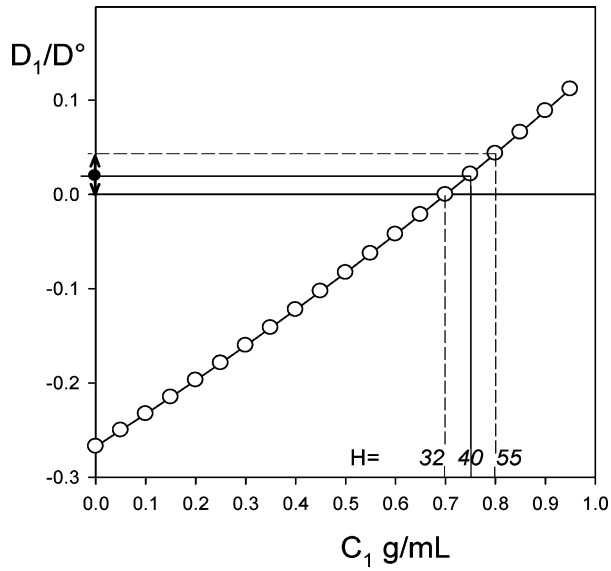

Figure 8. Mutual dependence of local self-diffusion coefficient (D_1) and concentration of water (C_1) to be used in eqs 4 and 5 in the case of spherical micelles made of only SDS ($D_W/D_W^\circ = 0.845$). Assuming a water/SDS mole ratio $H = 40$ ($C_1 = 0.75$ g/mL), the water diffusion is $D_1 = 0.021D_W^\circ$ (dot in the ordinate). Symmetric confidence intervals (double arrow on the ordinate) have been evaluated by assuming as natural lower limit $D_1 = 0$ and the corresponding $C_1 = 0.70$ g/mL ($H = 32$). Accordingly, the D_1 upper limit has been assumed to be $0.042D_W^\circ$ corresponding to $C_1 = 0.80$ g/mL ($H = 55$).

the cell has bulk concentration C_2 and self-diffusion coefficient D_2. The general equation has the form[33]

$$\frac{D^{cell}}{D_2} = \frac{U}{1 - \left(1 - \frac{C_1}{C_2}\right)\Phi} \tag{4}$$

where Φ is the micellar volume fraction, the function U depends on the C_1D_1 and C_2D_2 products and on the symmetry (shape of the micelles). For *spherical* micelles, taking into account that D_2 is the bulk diffusion ($D_2 = D_W^\circ$), eq 4 assumes, the simple form[33]

$$\frac{D_W}{D_W^o} = \frac{1}{1 - \left(1 - \frac{C_1}{C_2}\right)\Phi} \frac{1 - \beta\Phi}{1 + \beta\Phi/2} \tag{5}$$

where $\beta = (C_2D_2 - C_1D_1)/(C_2D_2 - {}^1/_2C_1D_1)$. Equation 5 is the closed solution for spherical micelles but it is also numerically indistinguishable from the solution obtained in the case of prolate and cylindrical micelles.[33,35,36] On the contrary, oblate and disklike micelles behave very differently.[33,35,34] Thus eq 5 could be used to check if disklike micelles are present in solution. Among the parameters in eq 5, only the water bulk properties $C_2 = 1$ g/mL and $D_2 \equiv D_W^\circ = 2.3 \times 10^{-9}$ m^2 s^{-1} are known a priori. To estimate the average diffusion (D_1) and concentration (C_1) of water within the region surrounding the micelle, we have compared the value D_W/D_W° experimentally determined for a solution of SDS (13 wt %) in water (a case where the spherical morphology is well assessed) with eq 5 as follows. Using the experimental $D_W/D_W^\circ = 0.845$ and guessed values of C_1 the term β has been evaluated according eq 5. Then using the definition of β, D_1 has been evaluated. In Figure 8 the dependence of the calculated D_1 value on the assumed C_1 is drawn. Clearly, C_1 and D_1 are strongly correlated so that reasonable estimates of D_1 are required to evaluate an accurate value of C_1. $D_1 = 0$ represents a natural lower limit for the water diffusion within the hydration layer; inspection of Figure 8 reveals that this corresponds to $C_1 = 0.70$ g/mL (i.e., to a mole ratio H = (hydration water)/SDS = 32).[37] The amount of water interacting with the polar surface of SDS micelles has been the subject of a recent investigation using dielectric spectroscopy.[38] The authors reported that 40 water molecules per SDS molecule are present within the counterions' shell ($H = 40$) and this corresponds to $C_1 = 0.75$ g/mL. We have therefore chosen this value as the true value, and correspondingly, $D_1 = 0.021D_W^\circ$ was estimated. Assuming symmetric confidence intervals in the local concentration $C_1 = 0.75 \pm 0.05$ the upper limit for water diffusion in the hydration layer is $D_1 = 0.043D_W^\circ$ (see Figure 8 for a graphical representation of these calculations). Once the values $C_1 = 0.75$ g/mL and $D_1 = 0.021D_W^\circ$ have been obtained, eq 5 was used to predict the water diffusion of samples in presence of CAPB and LA under the assumption that the addition of the minority components does not change dramatically the hydration properties of the micellar wall. Such a prediction is compared with the experimental data in Figure 7 (dashed curve). It is clear that the mere small increase in volume fraction associated with the LA and CAPB loading does not account for the observed decrease in water diffusion.

To justify the drop in D_W/D_W°, one should invoke a transformation into oblate micelles (it is worth emphasizing that spherical and cylindrical micelles have the very same effect on the solvent diffusion). Such a change in the micellar shape is consistent with the increase in apparent viscosity (from 2.4 to 8.2 Pa s) and in the apparent hydrodynamic size (from 95 to 140 Å, see the surfactant diffusion in the next section) associated with the CAPB loading. Note that to justify the drop in water diffusion with a mere change in the hydration of the micellar wall, one should admit an astonishing large layer of water molecules with nonbulk properties ($H = 672$).[39] Since it is very unlikely that the presence of less than 0.3 molecules of LA per SDS molecule changes dramatically the amount of water bound to the micellar surface, we conclude that the decrease in D_W/D_W° observed upon addition of LA is due to a transition in micellar shape toward oblate micelles.

In the case of oblate micelles the water diffusion is still described by eq 4 but the form of the function $U(\rho)$ is more complicated than the spherical case (eq 5) and depends on the oblate spheroid axial ratio ρ.[33] The analytical form of $U(\rho)$ for the oblate case was proposed in ref 33 and is reported in the Appendix; comparison with numerical simulations have demonstrated that it describes accurately the obstruction effect up to volume fractions of 25%.[35] It is possible to compare the predictions of eq 4 and of $U(\rho)$ described in the Appendix with the experimental D_w/D_W° to extract the axial ratio of the oblate micelles. The procedure is schematically illustrated in Figure 9 where the dependence of D_w/D_W° on the micellar axial ratio is shown for the case of $\Phi = 0.16$ (relevant for formulations loaded with LA 1.7 wt %). The continuous curve was calculated assuming $C_1 = 0.75$ g/mL and $D_1 = 0.021D_W^\circ$ while the dashed lines represent calculation performed using the confidence intervals on C_1 and D_1 coming from the analysis of water diffusion in SDS micelles. Comparison with the experimental value $D_w/D_W^\circ = 0.73$ allows for the determination of the axial ratio expectation value $\rho = 7.3$ and of the lower and upper confidence intervals ($\rho = 6.7$ and $\rho = 8.2$, respectively). Using this procedure, it has been possible to evaluate the effect of LA

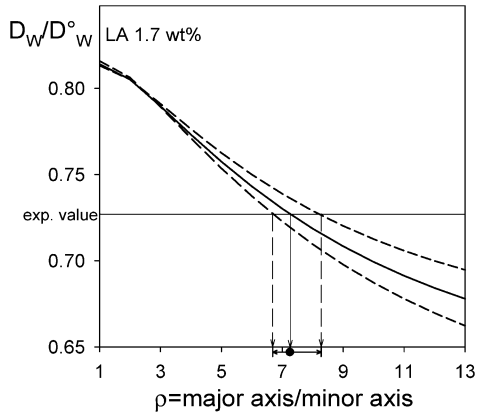

Figure 9. Determination of the axial ratio ρ for the sample with 1.7 wt % LA. The reduced water diffusion was evaluated for oblate micelles according to eqs A1−A7 in the Appendix by assuming the volume fraction of the sample ($\Phi = 0.16$) and different axial ratios. The solid curve assumes the water local self-diffusion coefficient ($D_1 = 0.021 D^{\circ}_W$) and concentration ($C_1 = 0.75$ g/mL) determined as in Figure 8. Comparison of the prediction with the experimental ratio $D_W/D^{\circ}_W = 0.73$ gives the ρ-value (dot on the abscissa). The dashed curves are the predictions for the D_1, C_1 pairs corresponding to the symmetric confidence intervals determined in Figure 8. Comparison of the experimental D_W/D°_W give the associated uncertainties (double arrow on the abscissa); note that these confidence intervals are asymmetric.

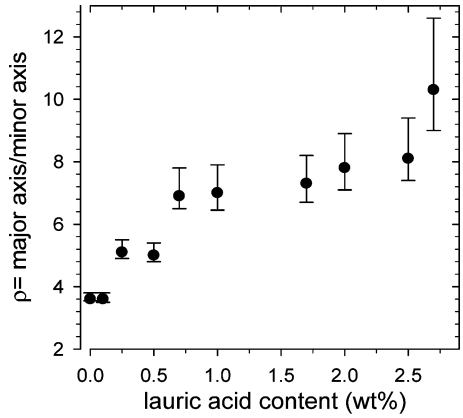

Figure 10. Dependence of the axial ratio of the oblate micelles on the LA content. The ρ-values and the associated uncertainties have been evaluated as described in Figure 9.

loading on the oblate micelles axial ratio (Figure 10). The full data set of Figure 7 can be consistently described in terms of a LA-induced two-dimensional growth of oblate micelles. At LA loading of 2.7 wt % the axial ratio is around 10 and the oblate micelles can be reasonably described as disks. It thus possible to use the relation between the volume fraction and axial ratio at the isotropic/nematic boundary valid for the Onsager treatment of disklike particles ($\Phi\rho = 2.1$)[29] to obtain a crude estimate of the axial ratio at the phase transition (i.e., at LA 2.7 wt %). The overall surfactant + LA volume fraction for formulation at 2.7% is $\Phi \approx 0.17$ and this leads to $\rho \approx 12$, in reasonable agreement with the independent treatment of water diffusion summarized in Figure 10. Finally, we spend some words on the diffusion of water in the nematic phase (data for LA > 2.7 wt % in Figure 7). The self-diffusion coefficients measured immediately after the insertion of the sample within the NMR probe (solid dots in Figure 7) indicate a further dramatic drop in the D_W/D°_W ratio. Presently, there are no theoretical models to describe the diffusion in a microdomain array of discotic (or columnar) nematic, but following the line of thought used in

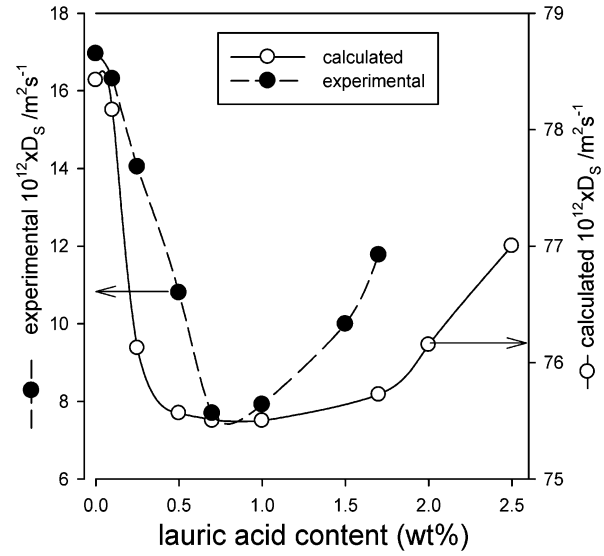

Figure 11. Surfactant self-diffusion coefficients as a function of the LA loading. The experimental values (●, left ordinate) are compared with the prediction for lateral diffusion of SDS (○, right ordinate) along oblate micelles with the axial ratios determined from the water diffusion (ρ-values in Figure 10). See text for details.

the analysis of the data in the isotropic phase, we suppose this is a consequence of a further increase of the axial ratio. Interestingly, when the nematic samples are allowed to equilibrate in the magnet, the water self-diffusion coefficients (asterisks in Figure 7) rise to the values expected for spheres/cylinders with the same hydration of SDS micelles (solid line in Figure 7). This is an independent demonstration that, as shown in section 3.3, the micelles orientate with their director normal to the magnetic field over the whole sample. Since the PGSE-NMR experiment probes the motion in the direction of the magnetic field, the water molecules experience as obstacles essentially the rims of the disks with an obstruction that is very similar to that brought about by rods.

3.5. Surfactant Diffusion. ^{1}H-PGSE-NMR experiments permitted us to probe the decay of the aliphatic signal up to a LA content of 2.0% only. For higher LA loading, the T_2 relaxation time was too short to observe any NMR signal attributable to components other than water. All the species SDS, CAPB, and LA contribute to the aliphatic resonance and in the following we label the corresponding self-diffusion coefficient as D_S because the most abundant species is the surfactant SDS. The experimental D_S values are shown in Figure 11 as a function of the LA content. In the absence of LA the surfactant self-diffusion coefficient is around 1.6×10^{-11} m^2 s^{-1} and decreases upon LA addition until a minimum in D_S is found at a content of LA of 0.7 wt %. For further loading with LA the D_S values increases.

In the following we will show how the monotonic increase in the micelles' axial ratio, inferred from the analysis of the water diffusion, semiquantitatively accounts for the peculiar minimum observed in the data of Figure 11. The ECM can be applied to model the diffusion of any components of a micellar solution, surfactant included.[33,34] The starting point is still eq 3, but in the case of the surfactant the micelle's diffusion cannot be neglected.

The diffusion of an oblate micelle at infinite dilution can be estimated from the Perrin equation

$$D^0_{mic} = \frac{k_b T}{6\pi\eta b} \cdot \frac{\arctan[\sqrt{\rho^2 - 1}]}{[\sqrt{\rho^2 - 1}]} \quad (6)$$

where b is the length of the micellar short semiaxis ($b \approx$ surfactant length ≈ 27 Å). At finite concentrations the micellar excluded volume reduces the diffusion coefficient due to the obstruction effect. To take into account this effect and estimate the micellar diffusion at finite concentration, the following equation has been proposed for nonionic systems[34]

$$D_{mic} = D^0_{mic}\left[1 - 2\frac{\Phi}{\rho^2}\left(\frac{\sqrt{\rho^2 - 1}}{\arctan[\sqrt{\rho^2 - 1}]}\right)^3\right] \quad (7)$$

As a whole, eqs 6 and 7 foretell a sizable decrease in the micellar diffusion as the axial ratio increases and thus a parallel drop in surfactant diffusion. However, for axial ratios large enough, the lateral diffusion within the aggregates as well as the reduction of the distance between the aggregates themselves contributes sufficiently to the macroscopic diffusion. The ECM implicitly accounts for this mechanism[33,34] because the reduction of the interaggregates distance corresponds to a reduction of the distance between the micelle and the cell boundary and a consequent increase in the term D_S^{cell} in eq 3. In principle, the combination of a decrease in D_{mic} and an increase in D_S^{cell} could give rise to a minimum in the measured diffusion upon increasing the axial ratio. To check if this could be the case, we have calculated the diffusion of the surfactant by combining eqs 3, 4, 6, and 7 and using reasonable estimates for the relevant parameters. The concentration of surfactant in the aqueous bulk phase was assumed equal to the critical micelle concentration (cmc) of SDS (because it is the main component of the surfactant mixture), i.e., $C_2 = 0.002$ g/mL. The self-diffusion coefficient in the bulk was assumed equal to that measured for a solution of SDS below the cmc (8×10^{-10} m^2 s^{-1}). The diffusion within the micelle was assumed to be $D_1 = 1.4 \times 10^{-10}$ m^2 s^{-1}, i.e., the value reported for lateral diffusion of SDS in hexagonal phases with decanol.[17] Finally, the concentration of SDS in the subvolume containing the micelle was evaluated by assuming 40 molecules of water per SDS molecule ($H = 40$) as done for the analysis of water diffusion. Using these parameters, the values of D_S have been calculated for each formulation, imposing the corresponding axial ratio values evaluated in section 3.4 (the ρ-values of Figure 10). The calculated values are compared to the experimental ones in Figure 11. It is clear that the simulation systematically overestimates the surfactant diffusion by a factor of 8 (note the different ordinates in Figure 11), but this is an acceptable discrepancy keeping in mind that the hollow dots in Figure 11 are the result of a true prediction without any adjustable parameters. In particular, the correction for the non-negligible concentration given by eq 7 is a very poor approximation for a charged system. This notwithstanding, the simulation successfully captures the order of magnitude of the diffusion coefficients and the minimum in the plot D_S vs lauric acid content and so can be considered an independent confirmation of the LA-induced growth of discrete disklike micelles.

4. Discussion

The addition of small quantities of LA to mixed solutions of SDS and CAPB has dramatic effects on the rheology and phase behavior (at almost constant volume fraction). Evidence from water diffusion (probed by PFG-NMR) and the results obtained with the ^{23}Na NMR spectroscopy clearly indicate a disklike shape of the micellar aggregates. The water diffusion was found to be progressively hindered upon LA loading. Since the amount of LA added is very small, hydration effects are expected to be negligible and an evolution of the shape of the micelles remains the only reasonable explanation. The strong decrease in the water diffusion cannot be explained by a one-dimensional growth into cylindrical wormlike micelles while two-dimensional growth is expected to strongly hamper the water diffusion. This point can be qualitatively understood by thinking about the limit cases of hexagonal and lamellar phases: in hexagonal phases the water is still able to diffuse in the 3-dimensions while in lamellar phases the diffusion along the direction parallel to the lamellae normal is hindered. On this basis, the evolution of the water self-diffusion coefficients was analyzed according to the effective cell model (ECM) and indicates that LA induced a dramatic increase in the aspect ratio ρ of the oblate micelle, which we estimate of about 10 at high LA content. Moreover the high aspect ratio (e.g., 10) reached around 2.7 wt % LA certainly would justify the ordering of the disklike micelles into a nematic phase based on disk-shaped micelles. The results of the ^{23}Na NMR experiment confirm that this mesophase is formed by the ordering of disklike micelles as elementary units. All the liquid crystalline samples show quadrupolar splitting with a line shape typical of monodomain samples (the intensity ratio of the three peaks is the canonical 3:4:3). Sample spinning, along a direction normal to the magnetic field, first destroys the alignment (only a single peak is discernible in the ^{23}Na NMR spectrum) then, upon prolonged spinning, develops again. This indicates that the nematic system is composed of disklike micelles that align themselves with their normal perpendicular to the magnetic field. On the other hand, the whole rheological response is reminiscent of a wormlike micellar solution. For the isotropic solutions in the presence of LA, the high viscosity and the dependence of G', G'' on the frequency is reminiscent of the single element Maxwell fluid response typically exhibited by wormlike micelles. In addition, we observe that also the minimum in surfactant diffusion coefficient (evident from Figure 11) is somehow reminiscent of wormlike micelles because for these systems "as a general feature, one observes a minimum of the diffusion coefficient as a function of surfactant concentration".[40]

Thus a first conclusion of the present study is a *caveat*: not always shear banding, huge viscosity, and single element Maxwell fluid response identify wormlike micelles.

The possible reasons for the apparently contradictory outcome of NMR and rheological measurements deserve some discussion. The shear banding plateau observed for samples with an LA content of 1.5 and 2.0 wt % can be attributed reasonably to a shear-induced isotropic-to-nematic transition, as supported by the presence of an adjacent isotropic−nematic transition, but this is independent from the kind of nematic phase. Nematics based on disklike micelles are good candidates as well as the calamitic nematic based on cylindrical micelles. The hypothesis of a phase based on rodlike micelles (calamitic nematic) can be ruled out on the basis of the NMR data (compatible only with a disklike micelles).

Another striking point is the huge viscosity attained by these disklike micelle solutions. For dilute suspensions the intrinsic viscosity of disklike colloids is much lower than that of rods (at the same volume fraction and aspect ratio) so that large viscosities cannot be attained (unless unphysical aspect ratios are admitted). However, the relevant volume fraction to define a dilute system is that of the excluded volume of the rotating

disk Φ_{EV}. If we assume oblate micelles with major semiaxis R and minor semiaxis d and with a volume $V_{mic} = (4/3)\pi R^2 d$, the excluded volume fraction is $\Phi_{EV} = (\Phi/V_{mic})(4/3)\pi R^3 = \Phi\rho$. The surfactant volume fraction is around $\Phi \approx 0.15$, and this means that, when the aspect ratio is close to 7, the volumes occupied by the rotating disks start to overlap. As shown in Figure 10, $\rho \approx 7$ takes place for a LA content between 1 and 2 wt %, i.e., where the maximum in viscosity is observed.

As stated above, for several systems of wormlike micelles the surfactant diffusion goes through a minimum as a function of the surfactant concentration.[40,41] This minimum results from the competition between two effects: the diffusion of the micelle itself (becoming hindered by an increase in the micelle size) and the surfactant molecule diffusion on the micelles (becoming significant upon an increase in the micellar size).[40] However, such interplay between diffusion *of* the micelle and diffusion *on* the micelle is not exclusive to wormlike (cylindrical) micelles. The same scenario holds for disks as well. Indeed, the ECM for disks successfully accounts for the minimum in Figure 11.

The crucial point in the rheological data consists in the development of a viscoelastic spectrum tending to that of a Maxwellian system. Usually this phenomenology is observed in wormlike micellar systems but the water diffusion unambiguously indicates the presence of disklike micelles in the isotropic phase. Such a nearly Maxwellian viscoelastic response seems to be incompatible with a random dispersion of disks, at least on the basis of the available theoretical descriptions. In contrast with the case of wormlike micelles, the rheology of disk-shaped objects has seldom attracted attention and only very simple models are available. It is thus possible that some details of the present system (e.g., long-range electrostatic forces, nonnegligible concentration and so on) bring about viscoelastic properties that are absent in the case of dilute hard disks.

An alternative explanation of the observed Maxwellian behavior is the presence of a local stacking of the disklike micelles in these isotropic solutions. If the length of the columnar stacks is large enough, they can meander as flexible objects and entangle, thus behaving as a "living" superassembly of discs, in analogy to the classical surfactant wormlike micelles, with the difference that now the dissociation and reassociation in a stack is caused by diffusion of single discotic micelles. Such a scenario is similar to what has been described in the case where some organogelators are based on disklike dendrimers[42] or bicopper tetracarboxilates.[43] Of course, this implies that the lyotropic mesophase found at LA contents higher than 2.7 wt % should not be the classical discotic nematic (N_D) but instead a nematic phase of aligned stacks of disks, without any lateral ordering of the stacks, the nematic columnar phase N_{Col}.[5] Since both the N_D and N_{Col} phases have the same symmetry, a similar ^{23}Na quadrupolar splitting and water diffusion is expected. Note that this *nematic columnar* phase N_{Col} must not be confused with the columnar phase, in which disklike micelles are packed in stacks, with no particular ordering along the stack, but there is lateral ordering (rectangular or hexagonal) of the columns in a lattice.[5] Nematic columnar phases are very common in liquid crystalline systems made of disklike molecules[5,44] for which the columnar nematic phase is stabilized by strong attractions, most commonly due to $\pi-\pi$ interactions or charge transfer interactions, but strong attractive interactions are absent in our system. Recently, evidence that the nematic columnar phase can be stabilized by the presence of weak attractions in a (dominantly) repulsive system has been reported. A nematic columnar (gel) phase has been experimentally observed in suspensions of charged hard disks (charge stabilized gibbsite platelets), occurring in a region of the phase diagram in which repulsive interactions dominate.[45] On the theoretical ground, it has been lately shown that soft disks (i.e., disklike particles with strong repulsion at short-range and weak attraction at long-range) in suitable solvent conditions spontaneously self-assemble into flexible stacks.[46]

Our results presented in the previous section and the literature results quoted above both suggest that it is conceivable that a nematic columnar phase can originate in a system of negatively charged disk-shaped micelles, probably stabilized by weak attractions.

As for the molecular origin of the disklike micellar shape, the growth of disklike micelles with an aspect ratio of approximately 7 takes place for a LA content between 1 and 2 wt %, i.e., where the maximum in viscosity is observed. This composition range corresponds to a mole ratio LA/CAPB of 0.5−1 and suggests that comparable amounts of betaine and fatty acid are required to induce a sizable anisotropic growth of the micelles. In the low concentration region of its phase diagram, SDS alone forms spherical micelles due to its packing parameter. However, the electrostatic interactions between SDS and CAPB in mixed micelles can decrease to some extent the spontaneous curvature of the surfactant film. This usually results in a transition toward elongated rodlike cylindrical micelles.[19] LA is not solubilized by SDS alone but it is incorporated by mixed micelles of SDS/CAPB; this suggests the presence of specific favorable interactions between LA and CAPB. It is thus conceivable that pairs CAPB-LA segregate from SDS rich regions within a micelle. A pair CAPB-LA is expected to confer a spontaneous curvature close to zero (it can be imagined as a sort of two-tails surfactant). On the other hand, $H_0 > 0$ for SDS. On these bases SDS is expected to concentrate on the edges of the aggregates shielding from the contact with water the central part of the micelle (rich in CAPB and LA) that has $H_0 \approx 0$.

In conclusion, addition of LA to the SDS and CAPB promotes the formation of disk-shaped micelles. The higher the LA content is, the higher the aspect ratio is until the system becomes a liquid crystalline phase with a nematic symmetry. The Maxwellian behavior experimentally observed in the viscoelastic response, just before the nematic transition, could be reconciled with the disk-shaped nature of the micelles by assuming the formation in the isotropic phase (for LA < 2.7 wt %), of entangled, flexible "living" columnar objects (composed by packed disklike micelles) and for the occurrence of an isotropic−nematic columnar transition at LA = 2.7 wt %. Further, work is needed to confirm the presence of such a hierarchical assembly of micelles and to clarify the intermicellar interactions.

Appendix. Self-Diffusion Coefficients in an Ensemble of Oblate Particles According to the ECM

In the original paper on the cell-diffusion model,[33] the two-region application described in section 3.3 was evaluated for a more general form in the case of a spheroidal cell containing a spheroidal particle. Since the particles are anisotropic, the tensor self-diffusion coefficient is now described by three components through a generalization of the eq 4 of the main text.

$$\frac{D_\kappa^{cell}}{D_2} = \frac{U_\kappa}{1 - \left(1 - \frac{C_1}{C_2}\right)\Phi_{eff}} \qquad \text{(A1)}$$

The subscript κ either represents the direction along the symmetry axis of the cell, in our case the z axis, or the direction perpendicular to the symmetry axis (note that by symmetry $D_x = D_y$). The two equations for U_κ, where $\kappa = z$ or $\kappa = x = y$ may be written as

$$U_z = 1 - \frac{\Phi}{\gamma - h(\xi_b) + \Phi h(\xi_R)}$$
$$U_x = 1 - \frac{2\Phi}{2\gamma - 1 + h(\gamma_b) + \Phi[1 - h(\xi_R)]} \quad \text{(A2)}$$

where ξ is the dimensionless spheroidal coordinate taking the value ξ_R at the cell boundary and ξ_b at the surface of the micelle. These values are determined by the aspect ratio ρ and volume fraction according to

$$\xi_b = \frac{1}{\sqrt{\rho^2 - 1}} \quad \text{(A3)}$$

$$\xi_R(\xi_R^2 + 1) = \frac{\xi_b(\xi_b^2 + 1)}{\Phi} \quad \text{(A4)}$$

The scale factor $h(\xi)$ entering eq A2 is

$$h(\xi) = (\xi^2 + 1)\cdot(1 - \xi \operatorname{arccoth} \xi) \quad \text{(A5)}$$

and the term γ, analogous to the parameter β in eq 5 of the main text, depends on the products C_1D_1 and C_2D_2 according to

$$\gamma = \frac{D_2C_2}{(D_2C_2 - D_1C_1)} \quad \text{(A6)}$$

Finally, if the directions of the prolate aggregates are isotropic, the average self-diffusion coefficient in the system becomes

$$D^{cell} = \frac{1}{3}D_z^{cell} + \frac{2}{3}D_x^{cell} \quad \text{(A7)}$$

Using eqs A1−A7 the effective self-diffusion coefficient in the cell was evaluated for different aspect ratios (ρ, entering eq A3) and then used to predict the macroscopic diffusion coefficient according to eq 3 of the main text.

Acknowledgment. This work was supported by University of Bari (prot. 23424 III/11 2009). G.P. and G.C. were supported by the Consorzio Interuniversitario per lo sviluppo dei Sistemi a Grande Interfase (CSGI-Firenze).

References and Notes

(1) Israelachvili, J. N. *Intermolecular and Surface Forces*, 2nd ed.; Academic Press: New York, 1992.
(2) Forrest, B. J.; Reeves, L. W. *Chem Rev* **1981**, *81*, 1.
(3) Boden, N.; Jolley, K. W.; Smith, M. H. *J. Phys. Chem.* **1993**, *97*, 7678.
(4) Kumar, S. *Liquid Crystals*; Cambridge University Press: Cambridge, U.K., 2001.
(5) Laschat, S.; Baro, A.; Steinke, N.; Giesselmann, F.; Hagele, C.; Scalia, G.; Judele, R.; Kapatsina, E.; Sauer, S.; Schreivogel, A.; Tosoni, M. *Angew. Chem. Int. Ed.* **2007**, *46*, 4832.
(6) Amaral, L. Q.; Helene, M. E. M. *J. Phys. Chem.* **1988**, *92*, 6094.
(7) Thiele, T.; Berret, J. F.; Mueller, S.; Schmidt, C. *J. Rheol.* **2001**, *45*, 1.
(8) Yu, L. J.; Saupe, A. *Phys. Rev. Lett.* **1980**, *45*, 1000.
(9) Braga, W.; Kimura, N. M.; Luders, D. D.; Sampaio, A. R.; Santoro, P. A.; Palangana, A. J. *Eur. Phys. J. E* **2007**, *24*, 247.
(10) Gosh, S. K.; Rathee, V.; Krishnaswamy, R.; Raghunathan, V. A.; Sood, K. *Langmuir* **2009**, *25*, 8497.
(11) Marcotte, I.; Auger, M. *Concept Magn. Reson. A* **2005**, *24A*, 17.
(12) Prosser, R. S.; Evanics, F.; Kitevski, J. L.; Al-Abdul-Wahid, M. S. *Biochemistry* **2006**, *45*, 8453.
(13) Johannesson, H.; Furo, I.; Halle, B. *Phys. Rev. E* **1996**, *53*, 4904.
(14) Furo, I.; Halle, B. *Phys. Rev. E* **1995**, *51*, 466.
(15) Halle, B.; Quist, P. O.; Furo, I. *Phys. Rev. A* **1992**, *45*, 3763.
(16) Quist, P. O.; Halle, B.; Furo, I. *J. Chem. Phys.* **1992**, *96*, 3875.
(17) Quist, P. O.; Halle, B.; Furo, I. *J. Chem. Phys.* **1991**, *95*, 6945.
(18) Furo, I.; Halle, B.; Quist, P. O.; Wong, T. C. *J. Phys. Chem.* **1990**, *94*, 2600.
(19) Christov, N. C.; Denkov, N. D.; Kralchevsky, P. A.; Ananthapadmanabhan, K. P.; Lips, A. *Langmuir* **2004**, *20*, 565.
(20) Stilbs, P. *Prog. NMR Spectrosc.* **1987**, *19*, 1.
(21) Tanner, J. E.; Stejskal, E. O. *J. Chem. Phys.* **1968**, *49*, 1768.
(22) The fraction of laurate at pH = 6 is expected to be negligible (the pK_a of LA is around 8).
(23) Cates, M. E. Theoretical modelling of viscoelastic phases. In *Structure and flow in surfactant solutions*; Herb, C. A., Prud'homme, R. K., Eds.; American Chemical Society: Washington, DC, 1994; p 32.
(24) Cates, M. E.; Fielding, S. Theoretical Rheology of Giant Micelles. In *Giant Micelles, properties and applications*; Zana, R., Kaler, E. W., Eds.; Taylor & Francis: Boston, 2007; p 109.
(25) Lequeux, F.; Candau, S. J. Dynamical properties of Wormlike micelles. In *Structure and flow in surfactant solutions*; Herb, C. A., Prud'homme, R. K., Eds.; American Chemical Society: Washington, DC, 1994; p 51.
(26) Berret, J. F. Rheology of wormlike micelles: equilibrium properties and shear banding transitions. In *Molecular Gels*; Weiss, R. G., Terech, P., Eds.; Springer: Dordrecht, The Netherlands, 2006; p 667.
(27) Laszlo, P. *Angew. Chem., Int. Ed. Engl.* **1978**, *17*, 254.
(28) Pound, R. V. *Phys. Rev.* **1950**, *79*, 685.
(29) de Gennes, P. G. *The Physics of Liquid Crystals*; Oxford University Press: London, 1974.
(30) Tan, C. B.; Fung, B. M.; Cho, G. J. *J. Am. Chem. Soc.* **2002**, *124*, 11827.
(31) Courtieu, J.; Bayle, J. P.; Fung, B. M. *Prog. Nucl. Magn. Reson. Spectrosc.* **1994**, *26*, 141.
(32) Radley, K.; Reeves, L. W.; Tracey, A. S. *J. Phys. Chem.* **1976**, *80*, 174.
(33) Jönsson, B.; Wennerström, H.; Nilsson, P. G.; Linse, P. *Colloid Polym. Sci.* **1986**, *264*, 77.
(34) Jonströmer, M.; Jönsson, B.; Lindman, B. *J. Phys. Chem.* **1991**, *95*, 3293.
(35) Johannesson, H.; Halle, B. *J. Chem. Phys.* **1996**, *104*, 6807.
(36) Murgia, S.; Palazzo, G.; Mamusa, M.; Lampis, S.; Monduzzi, M. *J. Phys. Chem. B* **2009**, *113*, 9216.
(37) C_1 = (H_2O grams)/(volume of the region surrounding the micelle); thus $C_1 = H^*18/(v_{SDS} + Hv_W)$ where v_{SDS} and v_W are the molar volume of SDS and water (247 and 18 mL/mol, respectively).
(38) Buchner, R.; Baar, C.; Fernandez, P.; Schrodle, S.; Kunz, W. *J. Mol. Liq.* **2005**, *118*, 179.
(39) This value was calculated by applying eq. 5 to the $D_W/D_W^0 = 0.80$ measured for the formulation containing SDS 11.5 wt % and CAPB 2.9 wt %, in other words, by assuming that in that sample the micelles are nonoblate. It turned out that to have a non-negative D_1 value one should admit $C_1 = 0.98$ g/mL.
(40) Schmitt, V.; Lequeux, F. *Langmuir* **1998**, *14*, 283.
(41) Lo Nostro, P.; Murgia, S.; Lagi, M.; Fratini, E.; Karlsson, G.; Almgren, M.; Monduzzi, M.; Ninham, B. W.; Baglioni, P. *J. Phys. Chem. B* **2008**, *112*, 12625.
(42) Yan, J.-J.; Tang, R.-P.; Zhang, B.; Zhu, X.-Q.; Xi, F.; Li, Z.-C.; Chen, E.-Q. *Macromolecules* **2009**, *42*, 8451.
(43) Terech, P.; Maldivi, P.; Dammer, C. *J. Phys. II* **1994**, *4*, 1799.
(44) Kumar, S. *Chem. Soc. Rev.* **2006**, *35*, 83.
(45) Mourad, M. C. D.; Byelov, D. V.; Petukhov, A. V.; Lekkerkerker, H. N. W. *J. Phys.: Condens. Matter* **2008**, *20*, 494201.
(46) Li, Z.-W.; Sun, Z.-Y.; Lu, Z.-Y. *J. Phys. Chem. B* **2010**, *114*, 2353.

JP1020774